274 *Chem. Mater.* **2011,** *23,* 274–284
DOI:10.1021/cm102975d

CHEMISTRY OF MATERIALS
Article

RGB Phosphorescent Organic Light-Emitting Diodes by Using Host Materials with Heterocyclic Cores: Effect of Nitrogen Atom Orientations

Shi-Jian Su,*[,†,‡] Chao Cai,[‡] and Junji Kido*[,‡]

[†]*Institute of Polymer Optoelectronic Materials and Devices, Key Laboratory of Specially Functional Materials of the Ministry of Education, South China University of Technology, Guangzhou 510640, China, and* [‡]*Department of Organic Device Engineering, Graduate School of Science and Engineering, Yamagata University, 4-3-16 Jonan, Yonezawa, Yamagata 992-8510, Japan*

Received October 15, 2010. Revised Manuscript Received December 5, 2010

A series of host materials **1**−**7** containing various heterocyclic cores, like pyridine, pyrimidine, and pyrazine, were developed for RGB phosphorescent organic light-emitting diodes (OLEDs). Their energy levels can be tuned by the change of heterocyclic cores and their nitrogen atom orientations, and decrease of singlet−triplet exchange energy (ΔE_{ST}) was achieved with introducing one or two nitrogen atoms into the central arylene; this is also consistent with density functional theory calculations. Their carrier mobilities can also be tuned by the choice of heterocyclic cores, giving improved bipolarity compared with that without any heterocyclic cores. Due to the high triplet energy level of the developed host materials, well confinement of triplet excitons of blue emitter iridium(III) bis(4,6-(difluorophenyl)pyridinato-$N,C^{2'}$) picolinate (FIrpic) was achieved except for **7** due to its low E_T. In contrast, triplet energy can be well confined on green emitter *fac*-tris-(2-phenylpyridine) iridium ($Ir(PPy)_3$) and red emitter tris(1-phenylisoquinolinolato-C^2,N)iridium-(III) ($Ir(piq)_3$) for all the hosts, giving comparable lifetime (τ), photoluminescent quantum efficiency (η_{PL}), and radiative and nonradiative rate constants (k_r and k_{nr}). Highly efficient blue and green phosphorescent OLEDs were achieved for **2**, exhibiting one of the highest ever efficiencies to date, especially at much brighter luminance for lighting applications. In comparison, the highest efficiencies hitherto were achieved for the red phosphorescent OLED based on **6**, which can be attributed to its lower-lying LUMO level and the smallest ΔE_{ST}, giving improved electron injection and carrier balance. Different from the blue and green phosphorescent OLEDs based on FIrpic and $Ir(PPy)_3$, the host materials with lower-lying LUMO levels seem to be better hosts for a red emitter $Ir(piq)_3$, achieving improved efficiency and reduced efficiency roll-off at high current density.

Introduction

Since the development of transition metal complexes, like iridium and platinum, by Forrest and Thompson's groups, nearly 100% internal quantum efficiency of electroluminescence has been realized by harvesting both electrogenerated singlet and triplet excitons for emission from organic light-emitting diodes (OLEDs) which emit phosphorescence from their triplet states.[1−4] To achieve a highly efficient phosphorescent OLED, triplet emitters are normally doped into a host material to reduce concentration quenching. Development of effective host materials is thus of importance for efficient phosphorescent OLEDs. Generally, triplet excited states of the host materials should be higher than those of the triplet emitters to prevent reverse energy transfer from the guest back to the host and to effectively confine triplet excitons on the guest molecules.[5,6] To meet this requirement, π-conjugation of the host materials should be limited to achieve a triplet energy level higher than that of the triplet emitter. As an example, triphenyl silyl-containing wide-band-gap insulating host materials have been developed for the blue phosphorescent emitter.[7] However, increased operating voltage was obtained since the charge hopping in the emitting layer (EML) occurred between the adjacent dopant molecules. As thus, another requirement for a host material is its carrier transport property, and a lot of host materials were developed with building blocks of carbazole, a well-known electron donor.[8−12] However, this may induce an unbalanced carrier injection and transport into the EML and then limited device performance.

*To whom correspondence should be addressed. E-mail: mssjsu@scut.edu.cn; kid@yz.yamagata-u.ac.jp.

(1) Baldo, M. A.; O'Brien, D. F.; You, Y.; Shoustikov, A.; Sibley, S.; Thompson, M. E.; Forrest, S. R. *Nature* (*London*) **1998**, *395*, 151.
(2) Baldo, M. A.; Lamansky, S.; Burrows, P. E.; Thompson, M. E.; Forrest, S. R. *Appl. Phys. Lett.* **1999**, *75*, 4.
(3) Adachi, C.; Baldo, M. A.; Thompson, M. E.; Forrest, S. R. *J. Appl. Phys.* **2001**, *90*, 5048.
(4) Adachi, C.; Kwong, R. C.; Djurovich, P.; Adamovich, V.; Baldo, M. A.; Thompson, M. E.; Forrest, S. R. *Appl. Phys. Lett.* **2001**, *79*, 2082.
(5) Holmes, R. J.; Forrest, S. R.; Tung, Y.-T.; Kwong, R. C.; Brown, J. J.; Garon, S.; Thompson, M. E. *Appl. Phys. Lett.* **2003**, *82*, 2422.
(6) Tokito, S.; Iijima, T.; Suzuki, Y.; Kita, H.; Tsuzuki, T.; Sato, F. *Appl. Phys. Lett.* **2003**, *83*, 569.
(7) Ren, X.; Li, J.; Holmes, R. J.; Djurovich, P. I.; Forrest, S. R.; Thompson, M. E. *Chem. Mater.* **2004**, *16*, 4743.
(8) Shih, P.-I.; Chiang, C.-L.; Dixit, A. K.; Chen, C.-K.; Yuan, M.-C.; Lee, R.-Y.; Chen, C.-T.; Diau, E. W.-G.; Shu, C.-F. *Org. Lett.* **2006**, *8*, 2799.

 Published on Web 12/29/2010

To solve this problem, building blocks of the electron acceptor, including benzimidazole,[13−16] phosphine oxide,[17,18] triazine,[19−21] and oxadiazole,[22] were introduced to develop host materials with improved electron injection and transport. Most recently, some host materials with building blocks of both electron donor and acceptor, called bipolar host materials, were developed.[23−28] However, it is anticipated that the introduction of both the electron donor and acceptor to the host material may lead to an intramolecular charge transfer, resulting in reduction of the energy band gap of the molecule. Nevertheless, few works report on the effect of the structure of the electron donor or electron acceptor on properties of host materials and thus device performance, which is of importance to realize highly efficient phosphorescent OLEDs for illumination applications utilizing blue, green, and red triplet emitters.

In this article, we report on a series of host materials **1**−**7** with similar π conjugation containing the electron donor of carbazole. These host materials are molecularly different from each other in the number of nitrogen atoms and their orientations in the central arylenes. Their carrier mobilities and energy levels, including the highest occupied molecular orbital (HOMO), the lowest unoccupied molecular orbital (LUMO), and singlet and triplet energies, can be tuned by the number of nitrogen atoms and their orientations, giving improved bipolarity compared with that without any heterocyclic cores. Blue, green, and red phosphorescent OLEDs were fabricated with well-known triplet emitters of iridium(III) bis(4,6-(difluorophenyl)pyridinato-$N,C^{2'}$) picolinate (FIrpic), *fac*-tris(2-phenylpyridine) iridium ($Ir(PPy)_3$), and tris(1-phenylisoquinolinolato-C^2,N)iridium(III) ($Ir(piq)_3$), respectively. The effects of the central arylenes on their photophysical properties, electron/hole mobilities, and device performances were studied comprehensively.

Experimental Section

General. The ^{1}H and ^{13}C NMR spectra were recorded on a Varian 500 (500 MHz) spectrometer. Mass spectra were obtained using a JEOL JMS-K9 mass spectrometer. Differential scanning calorimetry (DSC) was performed using a Perkin-Elmer Diamond DSC Pyris instrument under nitrogen atmosphere at a heating rate of 10 °C min^{-1}. Thermogravimetric analysis (TGA) was undertaken using a SEIKO EXSTAR 6000 TG/DTA 6200 unit under nitrogen atmosphere at a heating rate of 10 °C min^{-1}. UV−vis spectra were measured using a Shimadzu UV-3150 UV−vis−NIR spectrophotometer. PL spectra were obtained using a FluoroMax-2 (Jobin-Yvon-Spex) luminescence spectrometer. Ionization potentials were determined by atmospheric ultraviolet photoelectron spectroscopy (Rikken Keiki AC-3). Time-resolved emission spectra of host materials were obtained at T = 4.2 K under excitation by a nitrogen laser (λ = 337 nm, 50 Hz, 800 ps pulses) combined with a streak scope C4334 (Hamamatsu) and a synchronous delay generator C4792-02 (Hamamatsu). In comparison, transient photoluminescence (PL) decays and the corresponding simultaneous PL spectra of the phosphorescent emitter-doped films were recorded at room temperature. For calculation of HOMO and LUMO energy levels, density functional theory (DFT) calculations were performed for optimized molecular structures and single-point energies at the B3LYP/6-31G(d) and B3LYP/6-311+G(d,p) levels, respectively, using a Gaussian suite of programs (Gaussian 03W). For calculation of ground states (S_0) and triplet excited states (T_1), optimized molecular structures and single-point energies were also calculated at the B3LYP/6-31G(d) and B3LYP/6-311+G(d,p) levels, respectively.[29]

Device Fabrication and Characterization. Phosphorescent OLEDs were grown on glass substrates precoated with a ∼110-nm-thick layer of indium−tin oxide (ITO) having a sheet resistance of 15 Ω/□. The substrates were cleaned with ultrapurified water and organic solvents and then dry-cleaned for 20 min by exposure to an UV−ozone ambient. To improve hole injection from the anode, poly(arylene amine ether sulfone)-containing tetraphenylbenzidine (TPDPES) doped with 10% (by weight) tris(4-bromophenyl) aminium hexachloroantimonate (TBPAH) was spun onto the

(9) Tsai, M.-H.; Hong, Y.-H.; Chang, C.-H.; Su, H.-C.; Wu, C.-C.; Matoliukstyte, A.; Simokaitiene, J.; Grigalevicius, S.; Grazulevicius, J. V.; Hsu, C.-P. *Adv. Mater.* **2007**, *19*, 826.
(10) Fukagawa, H.; Watanabe, K.; Tsuzuki, T.; Tokito, S. *Appl. Phys. Lett.* **2008**, *93*, 133312.
(11) Tsai, M.-H.; Ke, T.-H.; Lin, H.-W.; Wu, C.-C.; Chiu, S.-F.; Fang, F.-C.; Liao, Y.-L.; Wong, K.-T.; Chen, Y.-H.; Wu, C.-I. *ACS Appl. Mater. Interfaces* **2009**, *1*, 567.
(12) Tsai, M.-H.; Lin, H.-W.; Su, H.-C.; Ke, T. H.; Wu, C.-C.; Fang, F.-C.; Liao, Y.-L.; Wong, K.-T.; Wu, C.-I. *Adv. Mater.* **2006**, *18*, 1216.
(13) Chen, C.-H.; Huang, W.-S.; Lai, M.-Y.; Tsao, W.-C.; Lin, J. T.; Wu, Y.-H.; Ke, T.-H.; Chen, L.-Y.; Wu, C.-C. *Adv. Funct. Mater.* **2009**, *19*, 2661.
(14) Takizawa, S.-Y.; Montes, V. A.; Anzenbacher, P., Jr. *Chem. Mater.* **2009**, *21*, 2452.
(15) Ge, Z.; Hayakawa, T.; Ando, S.; Ueda, M.; Akiike, T.; Miyamoto, H.; Kajita, T.; Kakimoto, M. *Chem. Mater.* **2008**, *20*, 2532.
(16) Ge, Z.; Hayakawa, T.; Ando, S.; Ueda, M.; Akiike, T.; Miyamoto, H.; Kajita, T.; Kakimoto, M. *Adv. Funct. Mater.* **2008**, *18*, 584.
(17) Padmaperuma, A. B.; Sapochak, L. S.; Burrows, P. E. *Chem. Mater.* **2006**, *18*, 2389.
(18) Vecchi, P. A.; Padmaperuma, A. B.; Qiao, H.; Sapochak, L. S.; Burrows, P. E. *Org. Lett.* **2006**, *8*, 4211.
(19) Chen, H.-F.; Yang, S.-J.; Tsai, Z.-H.; Hung, W.-Y.; Wang, T.-C.; Wong, K.-T. *J. Mater. Chem.* **2009**, *19*, 8112.
(20) Inomata, H.; Goushi, K.; Masuko, T.; Konno, T.; Imai, T.; Sasabe, H.; Brown, J. J.; Adachi, C. *Chem. Mater.* **2004**, *16*, 1285.
(21) Rothmann, M. M.; Haneder, S.; Da Como, E.; Lennartz, C.; Schildknecht, C.; Strohriegl, P. *Chem. Mater.* **2010**, *22*, 2403.
(22) Leung, M.-K.; Yang, C.-C.; Lee, J.-H.; Tsai, H.-H.; Lin, C.-F.; Huang, C.-Y.; Su, Y. O.; Chiu, C.-F. *Org. Lett.* **2007**, *9*, 235.
(23) Su, S.-J.; Sasabe, H.; Takeda, T.; Kido, J. *Chem. Mater.* **2008**, *20*, 1691.
(24) Tao, Y.; Wang, Q.; Yang, C.; Wang, Q.; Zhang, Z.; Zou, T.; Qin, J.; Ma, D. *Angew. Chem., Int. Ed.* **2008**, *47*, 8104.
(25) Hsu, F.-M.; Chien, C.-H.; Shih, P.-I.; Shu, C.-F. *Chem. Mater.* **2009**, *21*, 1017.
(26) Jeon, S. O.; Yook, K. S.; Joo, C. W.; Lee, J. Y. *Adv. Funct. Mater.* **2009**, *19*, 3644.
(27) Jeon, S. O.; Yook, K. S.; Joo, C. W.; Lee, J. Y. *Adv. Mater.* **2010**, *22*, 1872.
(28) Chou, H.-H.; Cheng, C.-H. *Adv. Mater.* **2010**, *22*, 2468.
(29) Frisch, M. J.; Trucks, G. W.; Schlegel, H. B.; Scuseria, G. E.; Robb, M. A.; Cheeseman, J. R.; Montgomery, J. A., Jr.; Vreven, T.; Kudin, K. N.; Burant, J. C.; Millam, J. M.; Iyengar, S. S.; Tomasi, J.; Barone, V.; Mennucci, B.; Cossi, M.; Scalmani, G.; Rega, N.; Petersson, G. A.; Nakatsuji, H.; Hada, M.; Ehara, M.; Toyota, K.; Fukuda, R.; Hasegawa, J.; Ishida, M.; Nakajima, T.; Honda, Y.; Kitao, O.; Nakai, H.; Klene, M.; Li, X.; Knox, J. E.; Hratchian, H. P.; Cross, J. B.; Bakken, V.; Adamo, C.; Jaramillo, J.; Gomperts, R.; Stratmann, R. E.; Yazyev, O.; Austin, A. J.; Cammi, R.; Pomelli, C.; Ochterski, J. W.; Ayala, P. Y.; Morokuma, K.; Voth, G. A.; Salvador, P.; Dannenberg, J. J.; Zakrzewski, V. G.; Dapprich, S.; Daniels, A. D.; Strain, M. C.; Farkas, O.; Malick, D. K.; Rabuck, A. D.; Raghavachari, K.; Foresman, J. B.; Ortiz, J. V.; Cui, Q.; Baboul, A. G.; Clifford, S.; Cioslowski, J.; Stefanov, B. B.; Liu, G.; Liashenko, A.; Piskorz, P.; Komaromi, I.; Martin, R. L.; Fox, D. J.; Keith, T.; Al-Laham, M. A.; Peng, C. Y.; Nanayakkara, A.; Challacombe, M.; Gill, P. M. W.; Johnson, B.; Chen, W.; Wong, M. W.; Gonzalez, C.; Pople, J. A. *Gaussian 03*, revision D.01; Gaussian, Inc.: Wallingford CT, 2004.

Scheme 1. Synthetic Routes of the Host Materials 1−7a

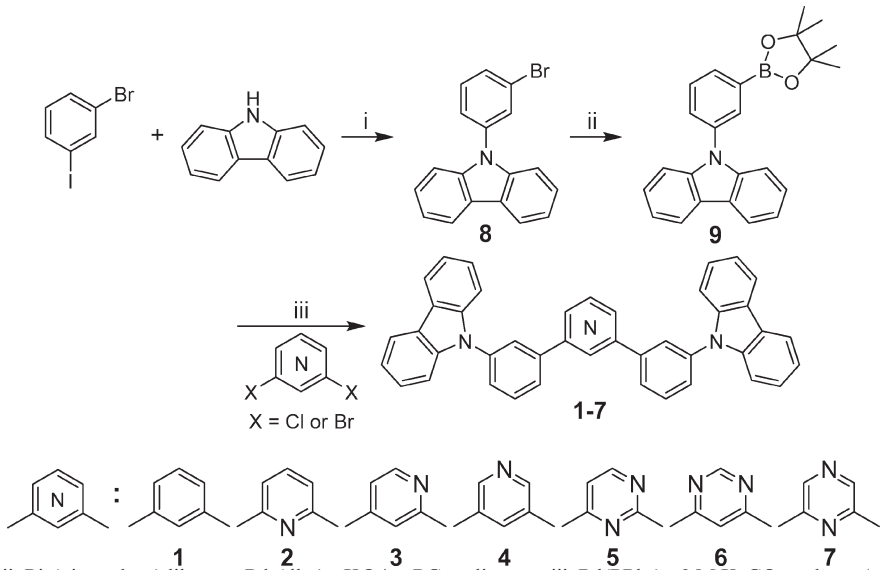

[a] i: Cu, K_2CO_3, DMF. ii: Bis(pinacolato)diboron, $Pd_2(dba)_3$, KOAc, PCy_3, dioxane. iii: $Pd(PPh_3)_4$, 2 M K_2CO_3, toluene/ethanol, or $PdCl_2(PPh_3)_2$, 2 M K_2CO_3, 1,4-dioxane, or $Pd_2(dba)_3$, PCy_3, K_3PO_4, 1,4-dioxane/water.

precleaned substrate from its dichloroethane solution to form a 20-nm-thick polymer buffer layer.[30] For the red phosphorescent OLEDs, a 35-nm-thick 1,1-bis(4-(*N*,*N*-di(*p*-tolyl)-amino)phenyl)-cyclohexane (TAPC) was deposited onto the buffer layer as a hole-transport layer (HTL). Then, 4% (by weight) $Ir(piq)_3$ was codeposited with the host materials to form a 10-nm-thick EML. Finally, a 65-nm-thick electron-transport layer (ETL) of 2,4,6-tris(3′-(pyridin-2-yl)biphenyl-3-yl)-1,3,5-triazine (TPyBPZ)[31] was deposited to block holes and to confine excitons in the emissive zone. For the green phosphorescent OLEDs, TAPC (30 nm), $Ir(PPy)_3$ (7 wt %):**1**−**7** (10 nm), and 1,3,5-tri(*p*-pyrid-3-yl-phenyl)benzene (TpPyPB)[32] (50 nm) were successively deposited as the HTL, EML, and ETL, respectively. 2,2′-Bis(*m*-di-*p*-tolyl-aminophenyl)-1,1′-biphenyl (3DTAPBP) (30 nm), Firpic (11 wt %):**1**−**7** (10 nm), and 3,5,3′,5′-tetra(*m*-pyrid-3-yl)phenyl-(1,1′)-biphenyl (TmPyPBP)[33] (40 nm) were successively deposited as the HTL, EML, and ETL, respectively, for the blue phosphorescent OLEDs. Cathodes consisting of a 0.5-nm-thick layer of LiF followed by a 100-nm-thick layer of Al were patterned using a shadow mask with an array of 2 × 2 mm openings. Electroluminescent (EL) spectra were taken by an optical multichannel analyzer, Hamamatsu PMA 11. Current density and luminance versus driving voltage characteristics were measured by Keithley source-measure unit 2400 and Konica Minolta chroma meter CS-200, respectively. External quantum efficiencies (η_{ext}) were calculated from the luminance, current density, and EL spectra, assuming a Lambertian distribution.

For carrier mobility measurement, films of **1**−**7** (∼10 μm) were prepared on ITO-coated substrates. A semitransparent Al layer was patterned using a shadow mask with an array of 2 × 2 mm openings. Hole/electron mobilities were measured by using a conventional photoinduced time-of-flight (TOF) technique. A nitrogen laser was used as the excitation source (λ = 337 nm) and was incident on the sample through the ITO or semitransparent Al electrode.

(30) Sato, Y.; Ogata, T.; Kido, J. *Proc. SPIE* **2000**, *4105*, 134.
(31) Su, S.-J.; Sasabe, H.; Pu, Y.-J.; Nakayama, K.-I.; Kido, J. *Adv. Mater.* **2010**, *22*, 3311.
(32) Su, S.-J.; Chiba, T.; Takeda, T.; Kido, J. *Adv. Mater.* **2008**, *20*, 2125.
(33) Su, S.-J.; Tanaka, D.; Li, Y.-J.; Sasabe, H.; Takeda, T.; Kido, J. *Org. Lett.* **2008**, *10*, 941.

Results and Discussion

Synthesis. The host materials were synthesized by Suzuki−Miyaura cross-coupling reaction between 9-(3-(4,4,5,5-tetramethyl-1,3,2-dioxaborolan-2-yl)phenyl)-carbazole (**9**) and aryl halide in the presence of palladium catalyst. **9** was synthesized by cross-coupling between bis(pinacolato)-diboron and 9-(3-bromophenyl)-carbazole (**8**), which was synthesized by Ullmann reaction between 1-bromo-3-iodobenzene and carbazole. Among these host materials, **1**, **2**, and **4** were synthesized with aryl bromide using tetrakis(triphenylphosphine)palladium(0) ($Pd(PPh_3)_4$) as the catalyst in the presence of 2 M K_2CO_3. In comparison, **5**, **6**, and **7** were synthesized with aryl chloride using bis(triphenylphosphine)palladium(II) chloride ($PdCl_2(PPh_3)_2$) as the catalyst. Taking into account the low reactivity of pyridine chloride, **3** was synthesized with 2,4-dichloropyridine using tris(dibenzylideneacetone) dipalladium(0) ($Pd_2(dba)_3$) as the catalyst in the presence of tricyclohexylphosphine (PCy_3) and K_3PO_4 (Scheme 1). All the host materials were obtained as white powders in good yields and were purified by repeated temperature gradient vacuum sublimation before characterization and device fabrication.

Physical and Optical Properties. UV−vis absorption and PL spectra of vacuum evaporated films (60 nm) for host materials **1**−**7** on quartz substrates measured at room temperature are shown in Figure 1. Their peak maxima are summarized in the Supporting Information, Table S1. Absorption peaks at 286, 297, 331, and 344 nm can be attributed to $\pi-\pi^*$ transitions of the carbazole chromophore. An absorption peak at around 243 nm and a shoulder at 265 nm can be attributed to $\pi-\pi^*$ and $n-\pi^*$ transitions of central arylenes, respectively. Absorbance at wavelengths longer than 350 nm increases with introducing one or two nitrogen atoms into the central arylenes. This can be attributed to strong electron affinity of heterocyclic arylenes and intramolecular charge transfer formed between the central heterocyclic arylenes and the

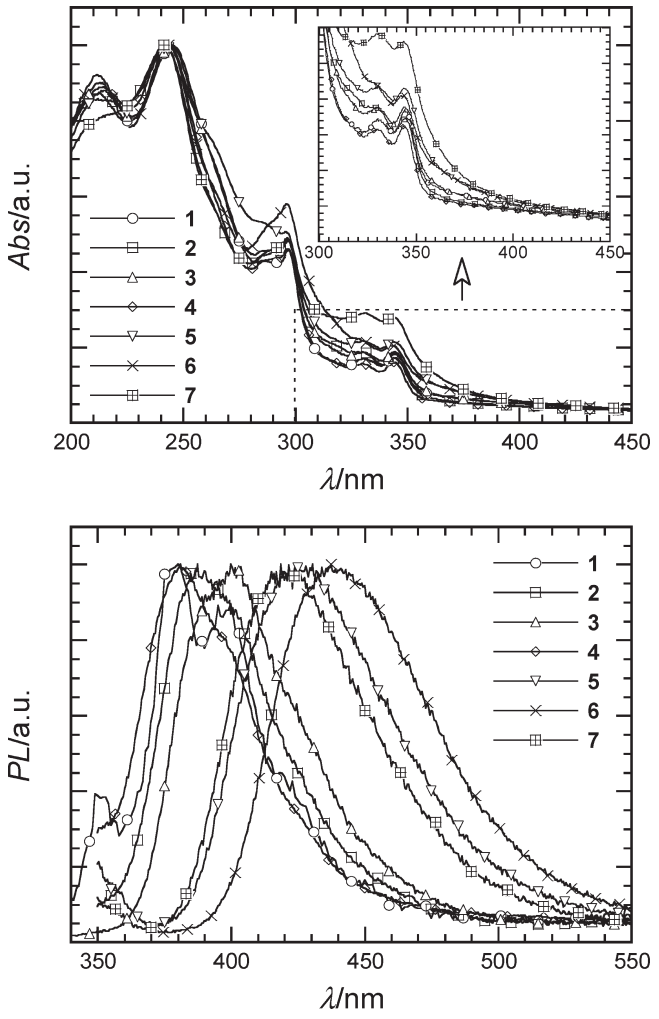

Figure 1. Room-temperature UV/vis absorption (top) and photoluminescence (bottom) spectra for vacuum-deposited films of host materials **1**−**7** on quartz substrates.

outer carbazoles. From their absorption edges, energy band gaps (E_g) of **1**−**7** can be assumed to be 3.48, 3.40, 3.38, 3.43, 3.17, 3.13, and 3.14 eV, respectively. As anticipated, narrower E_g values are obtained by introducing heterocyclic arylenes as the cores, and the more nitrogen atoms in the heterocyclic core, the narrower the E_g values obtained. For example, E_g of **2** is 3.40 eV, which is 0.23 and 0.26 eV wider than that of **5** and **7**, respectively. A similar phenomenon is also found for the other host materials.

PL spectrum of **1** peaks at 352, 378, and 400 nm. In contrast, PL spectra of **2**−**7** are structureless and peak at 387, 401, 381, 426, 439, and 421 nm, respectively. A bathochromic shift of the PL spectrum is found when introducing one or two nitrogen atoms in the central arylene core, and the more nitrogen atoms in the heterocyclic core, the longer the bathochromic shifts btained. Besides the number of nitrogen atoms, their PL spectra are also affected by nitrogen atom orientations in the heterocyclic cores. The host materials that have some nitrogen atoms at the *ortho*-position (refer to combination sites) show a longer bathochromic shift, and it can be attributed to elongated $n-\pi$ conjugation induced by nonpaired electrons of those nitrogen atoms.

HOMO energy levels of host materials **1**−**7** determined by atmospheric photoelectron spectroscopy are between 6.08 and 6.23 eV, and LUMO energy levels estimated from the corresponding HOMO and E_g are between 2.60 and 3.09 eV. As expected, lower-lying HOMO and LUMO energy levels are achieved by introducing heterocyclic cores with stronger electron affinity instead of benzene, and the more nitrogen atoms in the central heterocyclic core, the lower lying the HOMO and LUMO levels achieved. In addition, the orientations of nitrogen atoms in the heterocyclic cores also result in different energy levels, and one or more nitrogen atoms at the outside of the molecule seem to induce lower-lying energy levels. Besides host materials, a similar phenomenon has also been found for the pyridine-containing ETMs.[31,34]

To obtain triplet energies (E_T) of host materials **1**−**7**, extremely long PL decay components of their films lasting for ~10 ms were recorded at $T = 4.2$ K. Figure 2 shows two time-resolved emission spectra of each film. One is the emission spectrum obtained in the whole range ($0 < t < 10$ ms) (black lines), and the other is the emission spectrum of the delayed component ($2\text{ ms} < t < 10$ ms) (gray lines), also called the phosphorescence spectrum of the corresponding host material. **1**−**6** exhibit the highest-energy phosphorescence peaks ($S_0^{v=0} \leftarrow T_1^{v=0}$) at 456, 458, 458, 458, 461, and 470 nm, corresponding to E_T of 2.72, 2.71, 2.71, 2.71, 2.69, and 2.64 eV, respectively. Phosphorescence of **7** is too weak to estimate its peak or onset. Although phosphorescence of **2**−**4** with a pyridine core is slightly weaker than that of **1** with a benzene core, they show quite similar $S_0^{v=0} \leftarrow T_1^{v=0}$ and E_T. With introducing one more nitrogen atom in the central heterocyclic core, a bathochromic shift of phosphorescence was clearly seen, resulting in lower E_T for **5** and **6**. Although phosphorescence of **7** is too weak to estimate its peak or onset, it is anticipated that its E_T should also be lower than that of **1**−**4**. This will be proven by the following DFT calculations. Nevertheless, compared with a general host material of *N*,*N*′-dicarbazolyl-4,4′-biphenyl (CBP) ($E_T = 2.56$ eV), higher E_T can be achieved when the central arylenes between the outer carbazoles are combined with each other at their *meta*-positions (refer to combination sites).

Compared with the phosphorescence spectra, the stronger emission spectra at shorter wavelengths are due to fluorescence of the host materials, which are almost consistent with those recorded at room temperature. From the highest energy fluorescence peaks ($S_0^{v=0} \leftarrow S_1^{v=0}$), singlet energies ($E_S$) of host materials **1**−**7** can be estimated as 3.25, 3.10, 3.08, 3.14, 2.89, 2.82, and 2.94 eV, respectively. In addition to the requirement of a high E_T, a good host material is required to have favorable exchange energy as small as possible to allow for both charge injection into the host and efficient triplet emission from a dispersed triplet emitter. Here, the energy difference (ΔE_{ST}) between the singlet and triplet emission transitions is taken as an

(34) Su, S.-J.; Takahashi, Y.; Chiba, T.; Takeda, T.; Kido, J. *Adv. Funct. Mater.* **2009**, *19*, 1260.

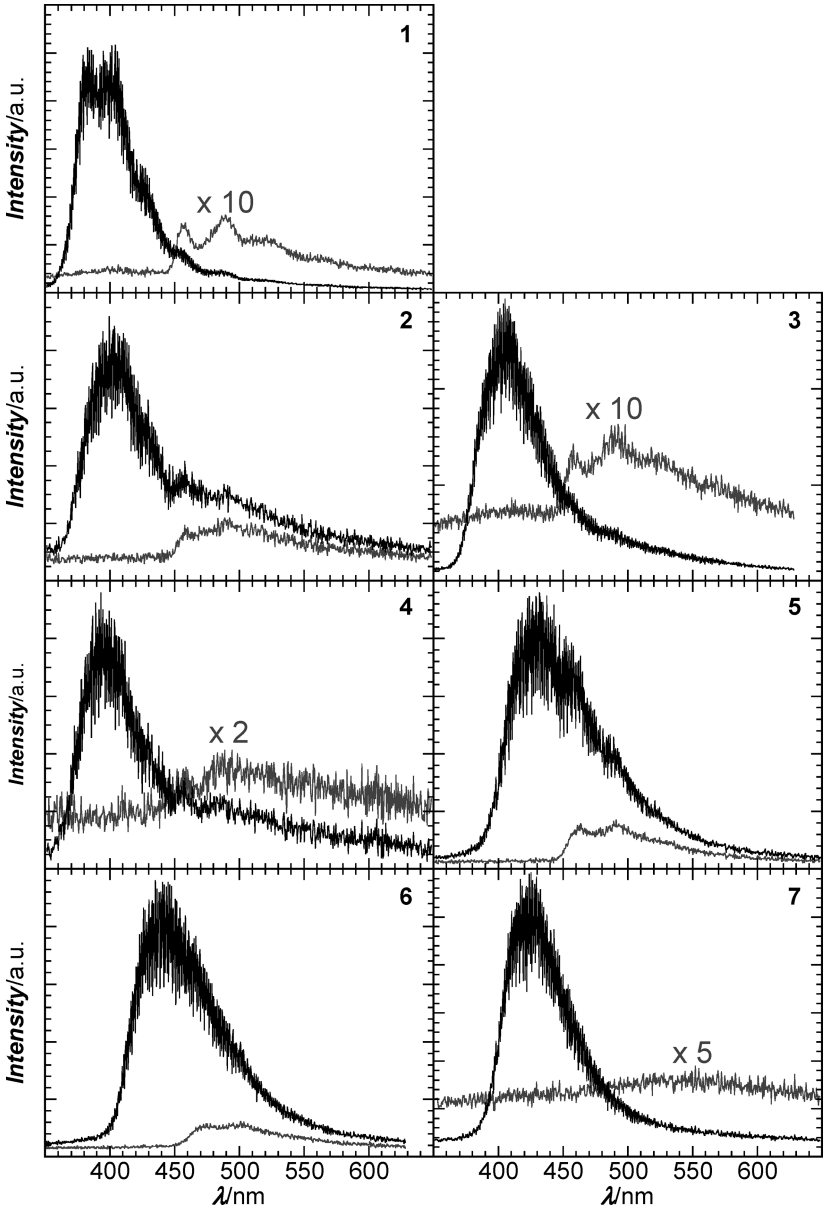

Figure 2. Time-resolved emission spectra of vacuum-deposited films of **1**−**7** excited by a nitrogen laser (λ = 337 nm, 50 Hz, 800 ps) at T = 4.2 K. Black lines: emission spectra in the whole range (0 < t < 10 ms). Gray lines: emission spectra of the delayed component (phosphorescence) (2 < t < 10 ms).

estimate for the exchange energy.[35] With introducing a pyridine core instead of a benzene core, a decrease of ΔE_{ST} by 0.10−0.16 eV (compare **1** and **2**−**4**) was achieved (Table 1). In addition, with introducing one more nitrogen atom into the central heterocyclic core, further decreases in ΔE_{ST} by 0.20 and 0.18 eV were achieved for **5** and **6**, respectively, indicating the host materials with heterocyclic cores may be attractive candidates to reduce the driving voltage of OLEDs.

Besides optical properties, their glass transition temperatures (T_g) are also influenced by the number of nitrogen atoms in the heterocyclic cores. Slightly improved T_g values are achieved for the host materials with one or two nitrogen atoms in the central arylene core, and it can be attributed to increased polarity and thus stronger molecular interaction. In addition, orientations of nitrogen atoms in the heterocyclic cores also affect their T_g. As an example, T_g values of **3** and **4** are slightly higher than that of **2** since their nitrogen atoms are located at the

Table 1. Singlet Energies (E_S, Measured as $S_0^{v=0} \leftarrow S_1^{v=0}$ at 4.2 K), Triplet Energies (E_T, Measured as $S_0^{v=0} \leftarrow T_1^{v=0}$ at 4.2 K), and Singlet−Triplet Energy Difference (ΔE_{ST}) for 1−7

materials	E_S, eV	E_T, eV	ΔE_{ST}, eV
1	3.25	2.72	0.53
2	3.10	2.71	0.39
3	3.08	2.71	0.37
4	3.14	2.71	0.43
5	2.89	2.69	0.20
6	2.82	2.64	0.18
7	2.94	n.a.	n.a.

(35) Brunner, K.; van Dijken, A.; Börner, H.; Bastiaansen, J. J. A. M.; Kiggen, N. M. M.; Langeveld, B. M. W. *J. Am. Chem. Soc.* **2004**, *126*, 6035.
(36) Meier, C.; Ziener, U.; Landfester, K.; Weihrich, P. *J. Phys. Chem. B* **2005**, *109*, 21015.
(37) Ziener, U. *J. Phys. Chem. B* **2008**, *112*, 14698.

outside of the molecule to give stronger molecular interaction than **2**, such as an intermolecular CH−N hydrogen-bonding interaction.[36,37] All the host materials show T_g higher than 100 °C, proving high morphologic stability of the amorphous phase in a deposited film, which is a prerequisite for their applications in OLEDs.

DFT Calculations. DFT calculations of **1**−**7** were performed using the Gaussian suite of programs (Gaussian 03W). To obtain their HOMO and LUMO energy levels, molecular structure optimization and single-point energy calculations were performed at the B3LYP/6-31G(d) and B3LYP/6-311+G(d,p) levels, respectively. As shown in Figure 3, HOMOs of all the host materials are mainly located at the outer carbazole. In contrast, their LUMOs are mainly located at the central diphenyl arylene skeleton between the outer carbazoles. The calculated HOMO and LUMO levels are demonstrated in the Supporting Information, Figure S1, in comparison with the experimental ones. It can be clearly seen that lower-lying LUMO energy levels are obtained by introducing heterocyclic cores instead of benzene, and the more nitrogen atoms in the heterocyclic core, the lower lying the LUMO levels obtained. Moreover, different energy levels are obtained by the change of nitrogen atom orientations in the heterocyclic cores. Although the experimental energy levels are somewhat different from the calculated ones, their trends are almost consistent. Different from the calculated LUMO levels, the calculated HOMO levels are slightly influenced by the number of nitrogen atoms and their orientations, and this is also consistent with the experimental results.

Triplet energies of **1**−**7** are obtained by the difference of their ground state (S_0) and triplet excited state (T_1) energies. Their optimized molecular structures and the corresponding single-point energies were also calculated at the B3LYP/6-31G(d) and B3LYP/6-311+G(d,p) levels, respectively. Although we failed in estimating E_T of **7** from its phosphorescence spectrum, the calculated one for **7** is 2.76 eV (Table 2), which is the lowest one among these host materials. It further proves that more nitrogen atoms in the central heterocyclic arylene induce lower triplet energies. Moreover, the trend of the calculated triplet energy is consistent with that of the experimental one. The energy difference (ΔE) between E_g and ($T_1 - S_0$) is taken as an estimate for the energy difference between the singlet and triplet transitions. Similar to the experimental ΔE_{ST}, ΔE of **1** with a benzene core is the largest one among these hosts, and smaller ΔE is achieved with introducing one or two nitrogen atoms in the central arylene core. In addition, ΔE of **6** is the smallest one among these hosts, which is also consistent with the experimental result.

Triplet Exciton Confinement. As a host material for a triplet emitter, its triplet excited state should be higher than that of the triplet emitter to prevent reverse energy transfer from the guest to the host. Since decreased E_T is obtained with introducing one or two nitrogen atoms in the central arylene, it seems in contradiction with this requirement. To verify their triplet exciton confinement

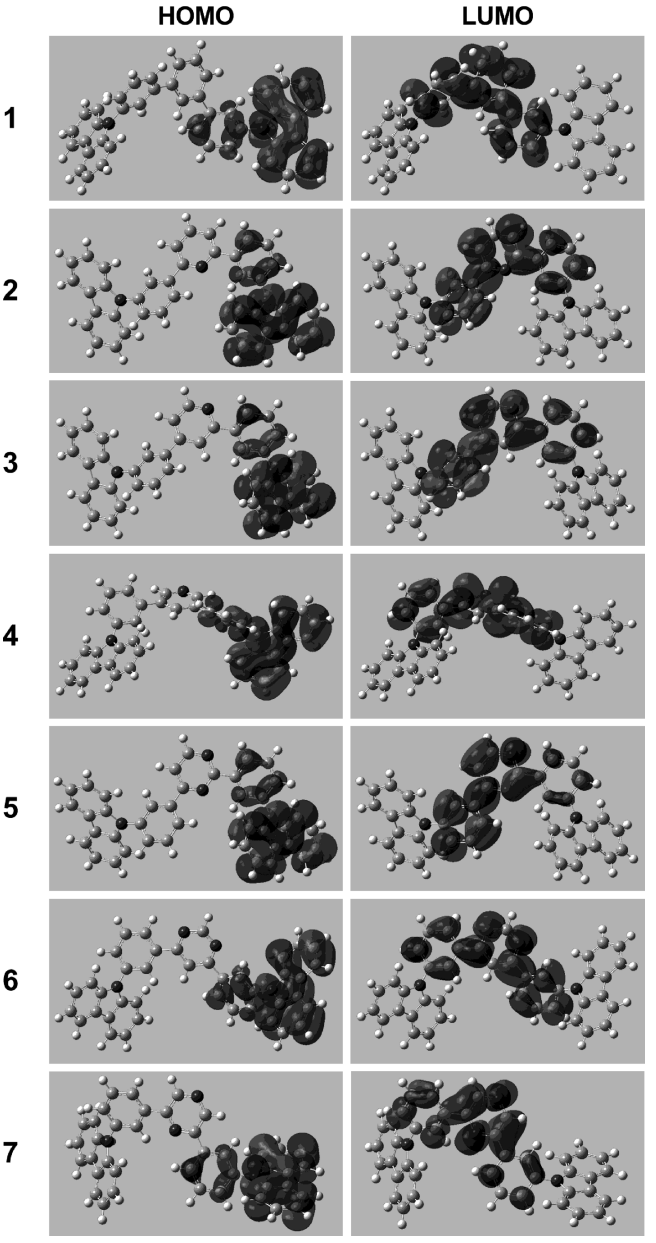

Figure 3. Calculated spatial distributions (DFT, B3LYP/6-311G+dp, Gaussian 03W) of HOMOs and LUMOs of **1**−**7**.

ability, well-known red, green, and blue triplet emitters of $Ir(piq)_3$, $Ir(PPy)_3$, and FIrpic were doped into **1**−**7** for transient PL decay measurements. Their decay curves and the corresponding simultaneous PL spectra were shown in Supporting Information, Figures S2−S4, respectively.

It can be seen that FIrpic doped into **1**−**4** and **6** clearly exhibits monoexponential decay curves with relatively long lifetimes between 1.51 and 1.73 μs (Table 3). In addition, they exhibit high PL quantum efficiency (η_{PL}) over 70%, which can be attributed to good confinement of triplet energy on the FIrpic molecules and efficient energy transfer from the host to the guest. Although transient PL decay of FIrpic doped into **5** is not monoexponential, its second exponential decay component is much smaller than its first one (lower than 1%), giving η_{PL} of 57% with a first exponential component lifetime of 1.29 μs. Among these host materials, FIrpic doped into **7**

Table 2. Density Functional Theory (DFT) Calculations of 1−7[a]

materials	HOMO, eV	LUMO, eV	E_g, eV	$T_1 - S_0$, eV	ΔE,[b] eV	dipole moment, D
1	5.72	1.60	4.12	2.95	1.17	1.460
2	5.69	1.89	3.80	2.84	0.96	3.008
3	5.73	2.04	3.69	2.86	0.83	1.481
4	5.77	1.78	3.99	2.93	1.06	2.455
5	5.69	2.30	3.39	2.82	0.57	1.622
6	5.73	2.42	3.31	2.78	0.53	2.150
7	5.78	2.28	3.50	2.76	0.74	1.588

[a] Molecular structure optimization and single-point energy calculations were performed at the B3LYP/6-31G(d) and B3LYP/6-311+G(d,p) levels (DFT, Gaussian 03W), respectively. [b] The energy difference (ΔE) between E_g and ($T_1 - S_0$) taken as an estimate for the energy difference between the singlet and triplet transitions.

Table 3. Phosphorescence Lifetime (τ), Photoluminescence Quantum Efficiency (η_{PL}), and Radiative and Nonradiative Rate Constants (k_r and k_{nr}) of FIrpic, Ir(PPy)$_3$, and Ir(piq)$_3$ Doped into 1−7

guests	hosts	τ, μs	η_{PL}, %	k_r, $\times 10^5$ s^{-1}	k_{nr}, $\times 10^5$ s^{-1}
FIrpic	**1**	1.51	83	5.48	1.13
	2	1.73	84	4.84	0.93
	3	1.53	71	4.65	1.90
	4	1.59	87	5.48	0.82
	5	1.29	57	4.41	3.32
	6	1.53	73	4.78	1.77
	7	0.67	18	2.67	12.2
Ir(PPy)$_3$	**1**	1.12	91	8.15	0.80
	2	1.24	85	6.86	1.22
	3	1.13	88	7.82	1.06
	4	1.24	90	7.28	0.81
	5	1.07	83	7.73	1.58
	6	1.23	87	7.10	1.06
	7	1.14	78	6.82	1.93
Ir(piq)$_3$	**1**	1.21	55	4.53	3.71
	2	1.19	53	4.46	3.95
	3	1.21	56	4.61	3.62
	4	1.23	55	4.49	3.67
	5	1.19	53	4.46	3.95
	6	1.23	56	4.57	3.59
	7	1.20	54	4.50	3.83

exhibits a complex decay curve with a short first exponential component lifetime of 0.67 μs. From its simultaneous PL spectrum, a high-energy emission peak was found at 425 nm, which can be attributed to delayed fluorescence of **7**, indicating inefficient energy transfer from **7** to FIrpic. Since the emissions from the host **7** and the guest FIrpic are covered with each other, the decay curve can be hardly devided according to the host or the guest, but the intensity from FIrpic is much stronger than that from the host. The first exponential component lifetime of 0.67 μs can be considered to be that of FIrpic. Besides the short lifetime, η_{PL} of FIrpic:**7** is only 18%, the lowest one among all the doped films. Moreover, its radiative rate constant (k_r) is only 2.67×10^5 s^{-1}, which is also the smallest one among these doped films and even much smaller than its nonradiative rate constant ($k_{nr} = 12.2 \times 10^5$ s^{-1}). All these results indicate E_T of **7** must be the lowest one among these host materials and should be equal to or lower than that of FIrpic ($E_T = 2.61$ eV, corresponding the highest-energy peak), further supporting the former experimental and calculation results.

In comparison, Ir(PPy)$_3$ doped into **1**−**7** clearly exhibits monoexponential decay curves with lifetimes between 1.07 and 1.24 μs. Their k_r values are between 6.82×10^5 and 8.15×10^5 s^{-1}, and k_{nr} values are between 0.80×10^5 and 1.93×10^5 s^{-1}. Both are slightly influenced by the different hosts compared with those for FIrpic. Ir(PPy)$_3$:(**1**−**6**) exhibit high η_{PL} over 80%. Even for **7** with the lowest E_T, η_{PL} of the doped film is as high as 78%, slightly lower than the others. It indicates good triplet energy confinement on the Ir(PPy)$_3$ molecules and efficient energy transfer from the host to the guest, and E_T of **7** should be higher than that of Ir(PPy)$_3$ ($E_T = 2.41$ eV, corresponding to the highest-energy peak).

For Ir(piq)$_3$ with the lowest triplet energy among these phosphorescent emitters, all the doped films exhibit clear monoexponential decay curves and relatively long lifetimes of about 1.2 μs. Their k_r values are between 4.46×10^5 and 4.61×10^5 s^{-1}, and k_{nr} values are between 3.59×10^5 and 3.95×10^5 s^{-1}. Their η_{PL} values are around 55% and are slightly affected by the number of nitrogen atoms and their orientations in the heterocyclic cores. The transient PL observation indicates that triplet energy transfer from Ir(piq)$_3$ to the hosts is completely suppressed, and the energy is well confined on the Ir(piq)$_3$ molecules due to their higher E_T than the guest.

Carrier Mobilities. Since the charge carriers are recombined in the EML in an OLED, balanced carrier injection and transport into the EML is a prerequisite for improved device performance. As thus, different from the hole-transport and electron-transport materials, balanced hole and electron mobility is ideal for a host material. Hole/electron mobilities of **1**−**7** were measured by using a conventional photoinduced TOF technique using a nitrogen laser as the excitation source ($\lambda = 337$ nm). Figure 4 shows their hole (μ_h) and electron (μ_e) mobilities plotted as a function of the square root of electric field (E). μ_h of **1** lies in the range from 9.6×10^{-5} to 1.8×10^{-4} cm^2 V^{-1} s^{-1} at an electric field between 3.0×10^5 and 7.2×10^5 V cm^{-1}, which is 1 order of magnitude higher than its μ_e, ranging from 1.1×10^{-5} to 5.2×10^{-5} cm^2 V^{-1} s^{-1} at an electric field between 3.6×10^5 and 8.1×10^5 V cm^{-1}. In contrast, μ_e values of **2**−**7** are somewhat higher or equal to their μ_h values except **6**, and the improved μ_e can be attributed to the heterocyclic cores with stronger electron affinity instead of benzene. Generally, μ_e of organic materials is several orders of magnitude lower than μ_h,[38] and as a host for the EML, increased μ_e may facilitate electron injection and transport into the EML to give a balanced carrier and thus higher recombination efficiency. μ_e of **6** is slightly

(38) Antoniadis, H.; Abkowitz, M. A.; Hsieh, B. R. *Appl. Phys. Lett.* **1994**, *65*, 2030.

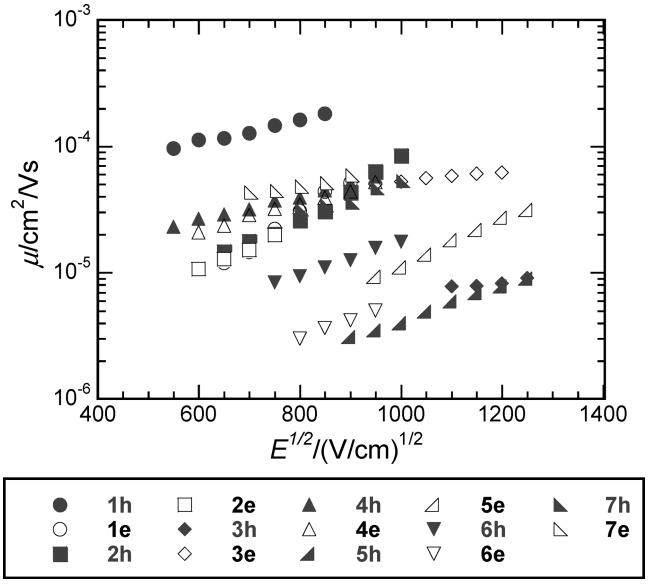

Figure 4. Hole (μ_h) and electron (μ_e) mobilities of **1**−**7** films plotted as a function of the square root of electric field (E).

lower than its μ_h, which can be attributed to its stronger molecular polarity since its two nitrogen atoms in the heterocyclic cores are located at the outside of the molecule.

μ_h of **1** is higher than that of **2**−**4**. In contrast, its μ_e is lower or equal to that of **2**−**4**. It can be seen that introducing the pyridine ring instead of benzene as the core induces lower μ_h but slightly affects μ_e. In addition, there is almost no effect on μ_e from the nitrogen atom orientation in the pyridine cores. A similar phenomenon has also been found for the pyridine-containing ETMs that their μ_e values are nearly independent of the nitrogen atom orientations.[34] Taking into account their energy levels and carrier mobility, an improved bipolarity has been achieved for the host materials containing heterocyclic cores compared with **1**.

Phosphorescent OLED Characterization. Blue, green, and red phosphorescent OLEDs were fabricated by doping FIrpic, $Ir(PPy)_3$, and $Ir(piq)_3$ into the developed host materials as the EMLs, and Figures 5−7 show their efficiency-luminance characteristics, respectively. Their performance data are summarized in Table 4. For the blue phosphorescent OLEDs, the highest efficiency was achieved for the host **2**, giving η_{ext} of 24.3% and power efficiency (PE) of 46.1 lm W^{-1} at 100 cd m^{-2} and rolling to 22.6% and 34.5 lm W^{-1} at 1000 cd m^{-2}, respectively, which is one of the highest performances for the FIrpic-based blue phosphorescent OLEDs.[32,34,39] In comparison, lower efficiencies of 21.3% and 40.2 lm W^{-1} were obtained at 100 cd m^{-2} for the host **1**. Although η_{PL} values of FIrpic:**1** and FIrpic:**2** are quite similar, the improved performance for the device based on **2** can be attributed to improved bipolarity of **2** achieving balance of electron and hole fluxes in the EML. For the devices based on **3** and **4** with the same pyridine core but different

(39) Su, S.-J.; Gonmori, E.; Sasabe, H.; Kido, J. *Adv. Mater.* **2008**, *20*, 4189.

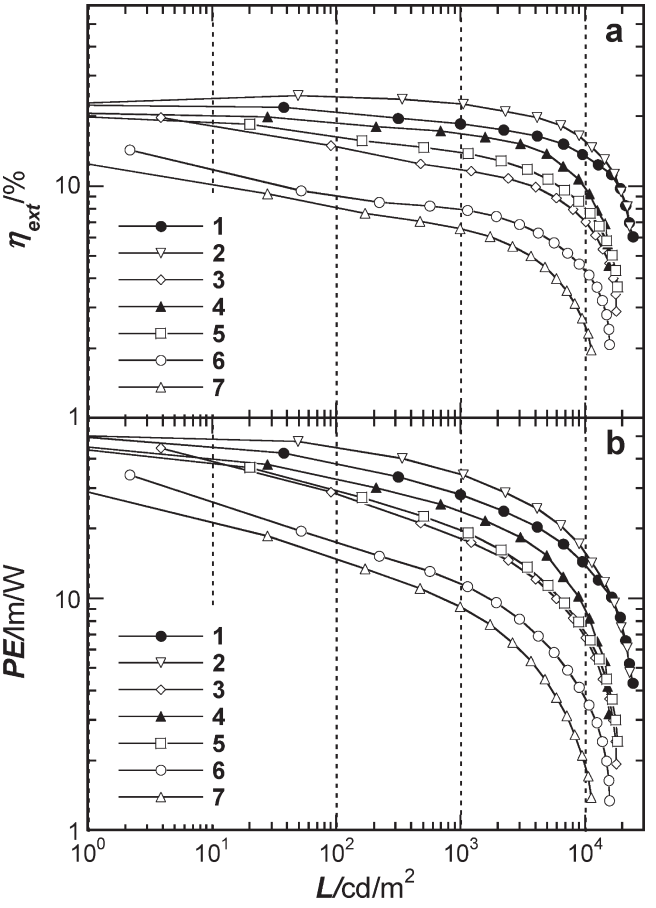

Figure 5. (a) External quantum efficiency (η_{ext}) and (b) power efficiency (PE) vs luminance (L) characteristics for ITO/TPDPES:TBPAH (20 nm)/3DTAPBP (30 nm)/**1**−**7**:11 wt % FIrpic (10 nm)/TmPyPBP (40 nm)/LiF (0.5 nm)/Al (100 nm).

nitrogen atom orientations, the efficiencies at 100 cd m^{-2} decreased to 14.9%, 28.6 lm W^{-1}, and 19.1%, 34.6 lm W^{-1}, respectively. Although η_{PL} of FIrpic:**4** is slightly higher than that of FIrpic:**2**, the decreased efficiency of the device based on **4** compared with the device based on **2** can be attributed to the lower-lying LUMO level of **4** giving electron-rich EML. Further reduced efficiency was obtained for the device based on **3** due to lower η_{PL} of FIrpic:**3**. η_{ext} values of the devices based on **5**−**7** decreased further to 16.9%, 9.2%, and 8.4%, respectively. As anticipated, efficiency of the device based on the host **7** is the lowest one among these host materials due to its lowest E_T and thus the lowest η_{PL}. Different from its PL spectrum, no emission from the host **7** was detected in the EL spectrum (Supporting Information, Figure S5), indicating some of the excitons are generated by a direct carrier trap by the FIrpic molecules. Since FIrpic is more like an electron transporter, a carrier trap by the FIrpic molecules may further induce unbalanced carriers in the EML containing host materials with low-lying LUMO levels.

For the green phosphorescent OLEDs, the highest efficiency was also achieved for the host **2**, exhibiting η_{ext} of 26.9% and PE of 102 lm W^{-1} at 100 cd m^{-2}. Although η_{PL} of $Ir(PPy)_3$:**1** is higher than $Ir(PPy)_3$:**2**, efficiencies of 22.0% and 83.6 lm W^{-1} were obtained at

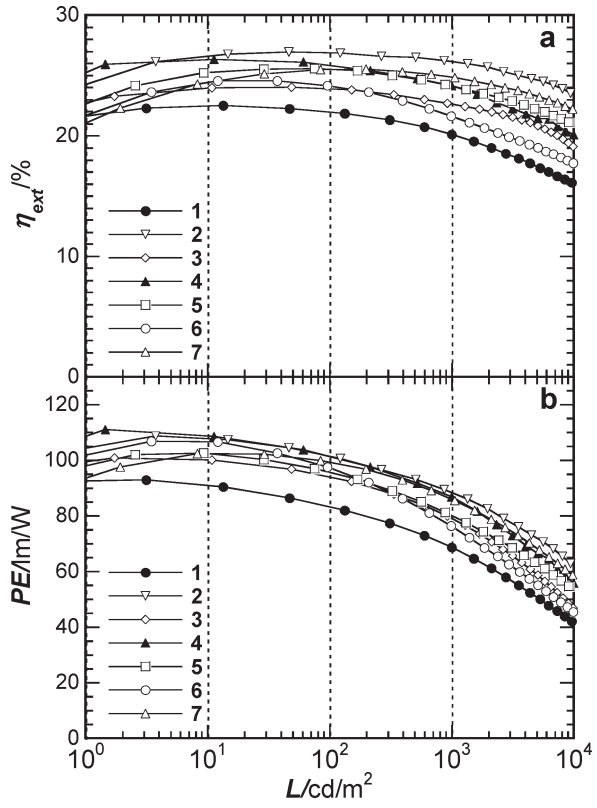

Figure 6. (a) External quantum efficiency (η_{ext}) and (b) power efficiency (PE) vs luminance (L) characteristics for ITO/TPDPES:TBPAH (20 nm)/TAPC (30 nm)/**1**−**7**:8 wt % Ir(PPy)$_3$ (10 nm)/TpPyPhB (50 nm)/LiF (0.5 nm)/Al (100 nm).

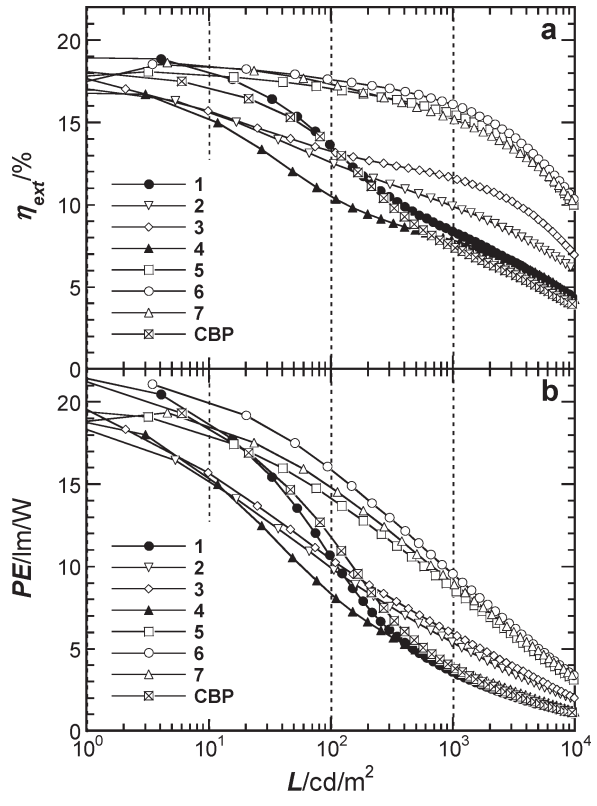

Figure 7. (a) External quantum efficiency (η_{ext}) and (b) power efficiency (PE) vs luminance (L) characteristics for ITO/TPDPES:TBPAH (20 nm)/TAPC (35 nm)/**1**−**7** or CBP:4 wt % Ir(piq)$_3$ (10 nm)/TPyBPZ (65 nm)/LiF (0.5 nm)/Al (100 nm).

100 cd m^{-2} for the device based on **1**, and both are the lowest one among these hosts. The improved efficiency for the host materials **2**−**7** can also be attributed to their improved bipolarity by introducing heterocyclic cores instead of benzene. Compared with the device based on **2**, slightly lower η_{ext} values of 23.9% and 25.9% were obtained at 100 cd m^{-2} for the devices based on **3** and **4** with the same pyridine core but different nitrogen atom orientations, but PE of the device based on **4** is as high as that of the **2**-based device at brightness lower than 200 cd m^{-2}. Besides the high efficiencies achieved by the host materials **2**−**7**, their η_{ext} values roll very slightly from a display-relevant luminance of 100 cd m^{-2} to an illumination-relevant luminance of 1000 cd m^{-2}. Even at a much brighter luminance of 10000 cd m^{-2}, η_{ext} remains 23.4% (corresponding to 83.9 cd/A) with a PE of 62.3 lm W^{-1} for the device based on **2**, and both are the highest ever values for the Ir(PPy)$_3$-based green phosphorescent OLEDs.[31−33] Besides **2**, η_{ext} values higher than 20% were also achieved at 10 000 cd m^{-2} for the devices based on **5** and **7**. It is of interest that all three host materials have a nitrogen atom located between the combination sites of the central heterocyclic core.

For the red phosphorescent OLEDs, all the devices show very high η_{ext} as 17%∼19% at low current density (∼0.01 mA cm^{-2}, luminance of ∼1 cd m^{-2} is detected). Note that η_{PL} values of Ir(piq)$_3$:**1**−**7** are around 55%. Taking into account that the light-out-coupling efficiency of an OLED is around 30%,[31,32] similar to the blue and green phosphorescent OLEDs, a well-balanced carrier was achieved at low current density for all the devices. With increase of current density, a steep decrease of η_{ext} was found for the device based on **1**. The steep decrease in η_{ext} can be attributed to reduced carrier balance at high current density. Note that the concentration of Ir(piq)$_3$ is as low as 4 wt %. At low current density, carriers may be injected into the EML through the Ir(piq)$_3$ dopant molecules, but at high current density, more carriers must be injected into the EML through the host molecules. Relatively high-lying HOMO and LUMO levels and the higher hole mobility of **1** facilitate hole injection and transport into the EML and thus a reduced carrier balance. The reduced carrier balance induces decreased carrier recombination efficiency and thus deduced η_{ext}. In addition, the imbalance of the carriers also causes domination of the hole polaron (h^+), and a large number of holes and polarons accumulate at the interface of EML and ETL and/or in the active layer, resulting in triplet exciton−polaron quenching and thus further efficiency roll-off.[40] On this result, η_{ext} rolls off to 8.36% at an illumination-relevant luminance of 1000 cd m^{-2}. Due to the high driving voltage at this luminance, PE further rolls off to 3.56 lm W^{-1}. As a control device based on a general host material CBP without any heterocyclic core, a similar steep decrease in η_{ext} and PE was also found due to this reason, and they are 7.44% and 3.86 lm W^{-1} at 1000 cd m^{-2}, respectively.

(40) Reineke, S.; Walzer, K.; Leo, K. *Phys. Rev. B* **2007**, *75*, 125328.

Table 4. Performance Data of RGB Phosphorescent OLEDs Using 1−7 as the Host Materials

		at 10 cd m^{-2}			at 100 cd m^{-2}			at 1000 cd m^{-2}		
guests	hosts	V, V	PE, lm W^{-1}	η_{ext}, %	V, V	PE, lm W^{-1}	η_{ext}, %	V, V	PE, lm W^{-1}	η_{ext}, %
FIrpic	**1**	3.13	48.5	22.2	3.61	40.2	21.3	4.50	28.0	18.6
	2	3.10	50.0	22.8	3.59	46.1	24.3	4.46	34.5	22.6
	3	3.05	42.9	19.3	3.51	28.6	14.9	4.35	18.5	11.9
	4	3.17	43.1	20.4	3.70	34.6	19.1	4.67	24.1	17.9
	5	3.24	42.0	19.5	3.78	31.2	16.9	4.88	19.9	14.0
	6	3.08	31.8	13.5	3.64	18.3	9.25	4.88	11.7	7.93
	7	3.17	26.2	11.6	3.75	15.9	8.43	5.00	14.6	6.55
Ir(PPy)$_3$	**1**	2.77	91.2	22.4	2.96	83.6	22.0	3.30	68.7	20.1
	2	2.76	108	26.5	2.97	102	26.9	3.33	88.4	26.2
	3	2.69	100	23.9	2.85	94.5	23.9	3.22	79.1	22.6
	4	2.69	109	26.3	2.82	102	25.9	3.10	86.8	24.2
	5	2.80	102	25.2	3.03	96.0	25.5	3.43	80.2	24.1
	6	2.58	106	24.3	2.80	97.3	24.1	3.20	76.2	21.6
	7	2.71	102	24.4	2.91	99.5	25.5	3.28	86.0	24.8
Ir(piq)$_3$	**CBP**	2.65	18.7	17.2	3.29	11.9	13.6	5.53	3.86	7.44
	1	2.70	19.0	18.2	3.62	10.6	13.6	6.62	3.56	8.36
	2	2.88	15.5	15.8	3.57	9.96	12.6	5.21	5.36	9.90
	3	2.80	15.7	15.7	3.55	10.5	13.2	5.50	5.92	11.6
	4	2.76	15.6	15.3	3.54	8.36	10.5	5.63	3.90	7.82
	5	2.71	18.2	17.9	3.30	14.2	17.1	4.92	8.65	15.5
	6	2.48	20.3	18.4	3.02	15.9	17.6	4.60	9.54	16.1
	7	2.66	18.8	18.5	3.15	14.9	17.3	4.56	9.00	15.2

Although efficiency roll-off was also found for the devices based on **2**−**4** with a pyridine core, it was suppressed compared with the devices based on CBP and **1**. Their η_{ext} values at 1000 cd m^{-2} luminance are 9.90%, 11.6%, and 7.82% with PEs of 5.36, 5.92, and 3.90 lm W^{-1}, respectively, which are improved in comparison to the devices based on CBP and **1**. The suppressed efficiency roll-off can be attributed to lower-lying energy levels and improved bipolarity of **2**−**4** compared with **1**, giving improved carrier balance and thus suppressed triplet exciton−polaron quenching at high current density.

Efficiency roll-off was further suppressed for the devices based on **5**−**7** with pyrimidine or pyrazine cores. Their η_{ext} values are 15.5%, 16.1%, and 15.2% at 1000 cd m^{-2} luminance, respectively, which are significantly improved in comparison to the devices based on CBP and **1**−**4**. As a factor concerning power consuming especially for high luminance applications, their PEs are improved to 8.65, 9.54, and 9.00 lm W^{-1} at 1000 cd m^{-2} luminance, respectively, and are over two times higher than those of the devices based on **1** and CBP. Moreover, decreased driving voltages were achieved for the devices based on **5**−**7** in comparison with those based on CBP and **1**−**4**, which can be attributed to their decreased ΔE_{ST} achieved with introducing one or two nitrogen atoms into the central arylene cores. This further proves that more carriers must be injected into the EML through the hosts rather than direct carrier trap by the dopant, especially at high current density. Taking the device based on **6** (ΔE_{ST} = 0.18 eV) as an example, the luminance reaches values of 10 and 100 cd m^{-2} at 2.48 and 3.02 V, respectively, which are even equal to or lower than those of the device based on a *p-i-n* structure.[41,42] η_{ext} and PE of 18.4% and 20.3 lm W^{-1} were achieved at 10 cd m^{-2} and slightly roll off to 17.6% and 15.9 lm W^{-1} at 100 cd m^{-2}. Both are the highest efficiencies for the red phosphorescent OLEDs based on Ir(piq)$_3$ hitherto.[41−44] Even at an illumination-relevant luminance of 1000 cd m^{-2}, the efficiencies maintain at 16.1% and 9.54 lm W^{-1}, respectively, compared with the highest ever values of 12.2% and 10.6 lm W^{-1} recorded at only 100 cd m^{-2}.[41] The suppressed efficiency roll-off can be attributed to low-lying LUMO levels of **5**−**7**, giving improved electron injection and carrier balance and thus reduced triplet exciton−polaron quenching at high current density. Different from the blue phosphorescent OLEDs based on FIrpic, the host materials with lower-lying LUMO levels seem to be better hosts for Ir(piq)$_3$ since FIrpic is a well-known electron-transport dopant and is more like a carrier trapper.

The emission color is deep red with an EL emission peak at 621 nm and CIE-1931 color coordinates of (0.673, 0.327), independent of the choice of hosts. This proves the emission directly from the triplet emitter Ir(piq)$_3$. Similar phenomena were also found for the blue and green phosphorescent OLEDs (Supporting Information, Figure S5). Note that the thickness of the current EMLs is only 10 nm, much thinner than in most of the phosphorescent OLEDs previously reported. Different from most of the efforts to reduce efficiency roll-off by using multi-EMLs to widen the carrier recombination zone,[45−47] the current study indicates that improved efficiency and reduced efficiency roll-off can be achieved for a device with a single EML and a narrow recombination zone by

(41) Meerheim, R.; Walzer, K.; He, G.; Pfeiffer, M.; Leo, K. *Proc. SPIE* **2006**, *6192*, 61920P.
(42) Meerheim, R.; Walzer, K.; Pfeiffer, M.; Leo, K. *Appl. Phys. Lett.* **2006**, *89*, 061111.
(43) Tsuzuki, T.; Tokito, S. *Adv. Mater.* **2007**, *19*, 276.
(44) Kanno, H.; Ishikawa, K.; Nishio, Y.; Endo, A.; Adachi, C.; Shibata, K. *Appl. Phys. Lett.* **2007**, *90*, 123509.
(45) He, G.; Pfeiffer, M.; Leo, K.; Hofmann, M.; Birnstock, J.; Pudzich, R.; Salbeck, J. *Appl. Phys. Lett.* **2004**, *85*, 3911.
(46) Watanabe, S.; Ide, N.; Kido, J. *Jpn. J. Appl. Phys., Part 1* **2007**, *46*, 1186.
(47) Sun, Y.; Forrest, S. R. *Appl. Phys. Lett.* **2007**, *91*, 263503.

the development of host materials with ideal energy levels.

Conclusions

We reported on a series of host materials containing building blocks of carbazole and arylenes, like benzene, pyridine, pyrimidine, and pyrazine. Their energy levels including HOMO, LUMO, singlet, and triplet energies can be tuned by the choice of central heterocyclic arylenes and also their nitrogen atom orientations, and this is also supported by the DFT calculations. A decrease of ΔE_{ST} was achieved with introducing one or two nitrogen atoms into the central arylene. Their carrier mobilities can also be tuned by different heterocyclic cores and nitrogen atom orientations, giving improved bipolarity. For the doped films FIrpic:**1**−**7**, triplet energy can be well confined on the guest molecules except for **7** due to its low E_T. In contrast, triplet energy can be well confined on Ir(PPy)$_3$ and Ir(piq)$_3$ molecules for all the hosts, giving comparable τ, η_{PL}, k_r, and k_{nr} slightly influenced by the heterocyclic arylenes. Highly efficient RGB phosphorescent OLEDs were fabricated with a single thin EML containing red, green, and blue phosphors of Ir(piq)$_3$, Ir(PPy)$_3$, and FIrpic and the developed hosts. One of the highest ever efficiencies to date was achieved for the blue and green phosphorescent OLEDs based on **2** with a pyridine core, especially at a much brighter luminance for lighting applications. In comparison, the highest efficiencies hitherto were achieved for the red phosphorescent OLEDs based on **6** with a pyrimidine core, which can be attributed to its low-lying LUMO level and the smallest ΔE_{ST}, giving improved electron injection and carrier balance and thus reduced triplet exciton−polaron quenching at high current density. Different from the blue and green phosphorescent OLEDs based on FIrpic and Ir(PPy)$_3$, the host materials with lower-lying LUMO levels seem to be better hosts for Ir(piq)$_3$ since more carriers must be injected through the host especially at high current density. To realize OLEDs for the next-generation illumination applications, development of highly efficient RGB triplet emitter-based phosphorescent OLEDs is the only route beyond fluorescent tube and inorganic LED efficacy. The current study gives an approach to such a goal by molecular design of host materials for specific triplet emitters.

Acknowledgment. This work was partly supported by the New Energy and Industrial Technology Development Organization (NEDO) through the "Advanced Organic Device Project". S.J.S. greatly appreciates the financial support from the National Natural Science Foundation of China (Project No. 51073057) and the Ministry of Science and Technology (Project No. 2009CB930604).

Supporting Information Available: Experimental procedures for the synthesis of **1**−**7**. Characterization data of **1**−**7** including EIMS and ^{1}H and ^{13}C NMR. Summary of physical properties of **1**−**7**. Calculated and experimental energy levels of **1**−**7**. Transient PL decays and simultaneous PL spectra of vacuum codeposited films of FIrpic:**1**−**7**, Ir(PPy)$_3$:**1**−**7**, and Ir(piq)$_3$:**1**−**7**. EL spectra of RGB phosphorescent OLEDs (PDF). This material is available free of charge via the Internet at http://pubs.acs.org.